Published in final edited form as:
Neurobiol Aging. 2010 June ; 31(6): 937–952. doi:10.1016/j.neurobiolaging.2008.07.006.

Age-related changes in glial cells of dopamine midbrain subregions in rhesus monkeys

Nicholas M. Kanaan[a], **Jeffrey H. Kordower**[a], and **Timothy J. Collier**[b]

[a]Rush University Medical Center, Department of Neurological Sciences, Chicago, Illinois, 60612, USA

[b]University of Cincinnati, Department of Neurology, Cincinnati, Ohio, 45267, USA

Abstract

Aging remains the strongest risk factor for developing Parkinson's disease (PD), and there is selective vulnerability in midbrain DA neuron degeneration in PD. By tracking normal aging-related changes with an emphasis on regional specificity, factors involved in selective vulnerability and resistance to degeneration can be studied. Towards this end, we sought to determine whether age-related changes in microglia and astrocytes in rhesus monkeys are region-specific, suggestive of involvement in regional differences in vulnerability to degeneration that may be relevant to PD pathogenesis. Gliosis in midbrain DA subregions was measured by estimating glia number using unbiased stereology, assessing fluorescence intensity for proteins upregulated during activation, and rating morphology. With normal aging, microglia exhibited increased staining intensity and a shift to more activated morphologies preferentially in the vulnerable substantia nigra-ventral tier (vtSN). Astrocytes did not exhibit age-related changes consistent with an involvement in regional vulnerability in any measure. Our results suggest advancing age is associated with chronic mild inflammation in the vtSN, which may render these DA neurons more vulnerable to degeneration.

Keywords

aging; Parkinson's disease; astrocyte; microglia; glia; midbrain; substantia nigra; ventral tegmental area; dopamine neuron; rhesus monkey; nonhuman primate; selective vulnerability

1. Introduction

Parkinson's disease (PD) is an age-related neurodegenerative disease characterized by the severe loss of dopamine (DA) neurons in the substantia nigra (SN). DA subregions in the midbrain exhibit differences in their susceptibility to degeneration (Gibb and Lees, 1991; Fearnley and Lees, 1991; Gibb, 1992; Damier et al., 1999; Kanaan et al. 2007). In PD, DA

Corresponding Author: Timothy J. Collier, PhD, Department of Neurology, University of Cincinnati, P.O. Box 670525, 265 Albert Sabin Way, Cincinnati, OH 45267, Telephone: 513-558-1168, Fax: 513-558-2965, timothy.collier@uc.edu.
Nicholas Kanaan: nicholas_kanaan@rush.edu
Jeffrey Kordower: jkordowe@rush.edu
Timothy Collier: timothy.collier@uc.edu

Disclosure Statement All of the authors report that there are no actual or potential conflicts of interest regarding this work.

neurons in the ventral tier of the SN (vtSN) are most vulnerable to degeneration, while those in the dorsal tier (dtSN) and ventral tegmental area (VTA) are more resistant to degeneration. It is becoming increasingly clear that changes associated with normal aging represent key components of the pathological processes that occur in PD. Recently, our group has shown that age-related reductions in DA phenotype (tyrosine hydroxylase-immunoreactivity (TH-ir)) follow regional patterns similar to those seen in PD, and these changes are associated with accumulation of intranuclear ubiquitin-positive inclusions and cytoplasmic non-aggregated soluble α-synuclein, in vulnerable DA neurons (Chu and Kordower, 2007; Kanaan et al., 2007). Given the proposed relationship between normal aging and PD, an approach that simultaneously evaluates normal aging and regional differences in vulnerability to degeneration represents a potent strategy towards understanding the factors involved in DA neuron degeneration. Although microglia and astrocytes have been implicated in the pathogenesis of PD (Vila et al., 2001; Hirsch et al., 2003; Teismann and Schulz, 2004), little is known concerning age-related changes in the glial environment of different midbrain DA subregions.

Microglia are considered the immune cells of the central nervous system. They produce cytokines and phagocytize cellular debris following injury (Aloisi, 2001). Microglial activation is characterized by morphological changes (e.g. increased cell soma size and shorter thicker cell processes), increased expression of certain proteins (e.g. class-II major histocompatibility complex glycoproteins (MHC-II) and cell surface receptors), and production of proinflammatory cytokines, among an array of other responses (van Rossum and Hanisch, 2004). Activation of microglia may play a pivotal role in DA neuron degeneration and the pathogenesis of PD (McGeer et al., 1988; Hunot and Hirsch, 2003; Kim and Joh, 2006). Normal aging is associated with increases in microglial activation most dramatically in white matter tracts, in addition to smaller changes in gray matter areas (e.g. cingulate and motor cortices, hippocampus, and striatum) (Perry and Gordon, 1991; Ogura et al., 1994; Sheffield and Berman, 1998; Sloane et al., 1999; Morgan et al., 1999). Little is known about normal age-related changes in microglia of midbrain DA subregions. We are aware of one study, which did not detect a change in number of activated microglia in the substantia nigra of middle-aged (12 month old) rats (Ogura et al., 1994). There are no studies in primates examining age-related changes in microglia of midbrain DA subregions with known differences in susceptibility to degeneration.

Astrocytes provide structural support, neurotrophic support, and serve to buffer ions and neurotransmitters in the extracellular environment in the central nervous system (Cotrina and Nedergaard, 2002). Glial fibrillary acidic protein (GFAP) is an intermediate filament in the cytoskeleton of astrocytes commonly used to identify astrocytes. In normal aging and in response to injury, astrocytes become reactive. With an increase in the expression of GFAP, activated astrocytes also display morphological changes such as swollen cell bodies and thickened processes, and enhanced production of cytokines and neurotrophic factors (Pekny and Nilsson, 2005). Normal aging has consistently been associated with increases in the amount of GFAP protein and GFAP mRNA in astrocytes in numerous brain regions such as the cortex, hippocampus, striatum, and cerebellum (Finch and Morgan, 1990; Cotrina and Nedergaard, 2002). Only a few studies have addressed age-related changes in GFAP-positive (GFAP+) astrocytes in the midbrain, and in these studies detailed analyses were not performed (Beach et al., 1989; Bronson et al., 1993). Furthermore, we are unaware of any studies describing age-related changes in astrocytes located within DA subregions with known differences in susceptibility to degeneration.

The current study was designed to determine the patterns of changes in microglia and astrocytes during normal aging in the midbrain of rhesus monkeys and to determine whether changes suggest a role for glial involvement in regional differences in susceptibility to degeneration.

Based on the association between normal aging and PD, we tested the hypothesis that aging-related changes in the glial environment that may participate in the pathogenesis of PD occur differentially in DA subregions with known patterns in selective vulnerability to degeneration. Specifically, we tested the hypotheses that during normal aging, microglial reactivity would be part of a deleterious process, thus occurring in the vulnerable vtSN region, while astrocyte reactivity would serve a protective role, thus occurring in the resistant dtSN and VTA regions. Glial reactivity was determined by quantifying the number of each cell type using unbiased stereological cell counting methods, measuring fluorescence intensity for human leukocyte antigen-DR protein (HLA-DR; an MHC-II glycoprotein) and GFAP immunoreactivity (-ir), and qualitatively rating established morphological characteristics of glia that correlate with activation state in the vtSN, dtSN, and VTA of young, middle-age, and old-age rhesus monkeys. We found that microglia exhibit age-related changes consistent with an involvement in the enhanced vulnerability of vtSN DA neurons, while changes in astrocytes did not suggest an involvement in vulnerability or resistance.

2. Materials and methods

2.1. Animals and tissue collection/preparation

Tissues from the same young male (9-10yrs, n=3), middle-aged male (14-17yrs, n=6), and old-aged female (22-29yrs, n=5) naïve rhesus monkeys described by Kanaan et al. (2007) were used in this study. The animals were born in captivity and were not used in previous studies. The current study was approved by the Institutional Animal Care and Use Committees of Rush University Medical Center and the Biological Research Laboratory at the University of Illinois at Chicago. All laws and regulations outlined in the National Institutes of Health, United States Public Health Service Guide for the Care and Use of Laboratory Animals were adhered to during the project. Tissue was collected and prepared for immunohistochemistry (IHC) and immunofluorescence as described previously (Kanaan et al., 2007). All samples were coded and analyzed by a blinded investigator.

2.2. Antibodies

The following primary antibodies were used to label microglia, astrocytes, and DA neurons, respectively: mouse anti-human B-lymphocyte clone LN-3 IgG_{2b} antibody (HLA-DR; MP Biomed, 693031, lot R13319), rabbit anti-cow GFAP antibody (Dako, Z0334, lot 00015316), and mouse anti-tyrosine hydroxylase (TH) IgG_1 antibody (Chemicon, MAB318). The mouse anti-human B-lymphocyte clone LN-3 monoclonal antibody was raised against the non-polymorphic HLA-DR (Ia-like) antigen and recognizes a band at 29-33 kDa in western blot preparations. HLA-DR is an MHC-II glycoprotein, which is integral in immune responses of microglia, and is commonly used to identify activated microglia with the ability to present antigens in humans and monkeys (Aloisi, 2001; Hurley et al., 2003). The rabbit anti-cow GFAP polyclonal antibody was generated against GFAP isolated from cow spinal cord. GFAP is considered one of the best markers for identifying astrocytes and determining astrocyte reactivity (Pekny and Nilsson, 2005). The mouse anti-TH antibody has been described in detail previously (Kanaan et al., 2007).

Since HLA-DR and TH antibodies are different IgG isotypes, isotype-specific secondary antibodies were used. The specificity of the isotype-specific antibodies was confirmed empirically using mismatched secondary antibodies. When the IgG_{2b} primary antibody (HLA-DR) was paired with the IgG_1 secondary, and when the IgG_1 primary antibody (TH) was paired with the IgG_{2b} secondary no staining was present (data not shown). These results confirmed the isotype-specific secondary antibodies did not cross-react with the other IgG isotype.

2.3. HLA-DR and GFAP IHC

Following a similar protocol to those previously published (Kanaan et al., 2006; Kanaan et al., 2007) a 1-in-12 series of tissue was processed for HLA-DR or GFAP IHC to label microglia and astrocytes for cell counting and morphological rating. In addition, sections containing cortex, putamen (post-commissural), globus pallidus (externa), and hippocampus (polymorphic layer) were stained for GFAP to confirm established patterns of age-related astrocytosis in these regions. Briefly, tissues were rinsed, incubated in H_2O_2 to block endogenous peroxidase (45 min), rinsed, incubated in blocking solution (10% goat serum (GS)/ 2% bovine serum albumin/0.5% Triton-X 100 tris buffered saline (TBS)), and incubated in primary antibody (72 hrs at 4° C). Microglia were labeled using mouse anti-HLA-DR primary antibody (1:200) diluted in 2% GS/TBS. Astrocytes were labeled using rabbit anti-GFAP primary antibody (1:50,000) diluted in 2% GS/TBS. Sections were then rinsed, incubated in biotinylated goat anti-mouse secondary antibody (for microglia - 1:400; Vector, BA-9200) or biotinylated goat anti-rabbit secondary antibody (for astrocytes - 1:400; Vector, BA1000), rinsed, incubated in avidin-biotin complex solution (Vector, PK-6100), and rinsed. All tissue was simultaneously reacted with 3,3-diaminobenzidine tetrahydrochloride (Sigma, D5637) enhanced with 2% nickel ammonium sulfate (Fisher, N48-500). After rinsing, sections were mounted on gelatin-coated microscope slides and allowed to air dry overnight. Once dry, the sections were rinsed in dH_20, counterstained for Nissl using 1% cresyl violet, rinsed in H_2O, dehydrated through graded ethanol (50, 70, and 95%), rinsed in 95% ethanol/1.4% glacial acetic acid solution (1-1.5 min), further rinsed in ethanols (95% and 99%), and cleared in xylenes. Sections were then coverslipped using Cytoseal 60. Penetration of immunohistochemical staining for HLA-DR and GFAP throughout the entire z-axis of the tissue sections was confirmed prior to analysis.

2.4. Stereology

The number of HLA-DR+ microglia and GFAP+ astrocytes were quantified in the vtSN, dtSN, and VTA of young, middle-aged, and old-aged monkeys using stereological cell counting techniques. The optical fractionator probe was used to estimate total number of glia in each region as previously published (Kanaan et al., 2007). Briefly, the system was composed of an Olympus BX52 microscope (Olympus America Inc., Melville, NY), Ludl motorized stage, Stereo Investigator version 7.0 software (MicroBrightField, Williston, VT), and a Microfire CCD camera (Optronics, Goleta, CA). The vtSN, dtSN, and VTA were outlined at low magnification (1.25x). For microglia, the counting frame size was 100μm × 75μm × 13 μm and the sampling grid size was 525μm × 413μm for the vtSN, 190μm × 146μm for the dtSN, and 230μm × 244μm for the VTA. This corresponds to sampling 3.5%, 27%, 13% of the area or 0.23%, 0.99%, and 0.72% of the entire volume of the vtSN, dtSN, and VTA, respectively. On average, 220, 80, and 170 microglia were counted in the vtSN, dtSN, and VTA, respectively. For counting astrocytes, the counting frame size was 100μm × 75μm × 13 μm and the sampling grid size was 740μm × 570μm for the vtSN, 310μm × 240μm for the dtSN, and 360μm × 510μm for the VTA. This corresponds to sampling approximately 2%, 10%, and 4% of the area or 0.05%, 0.36%, and 0.12% of the entire volume of the vtSN, dtSN, and VTA, respectively. On average, 290, 130, and 160 astrocytes were counted in the vtSN, dtSN, and VTA, respectively. The Gundersen method for calculating the coefficient of error (CE) was used to estimate the accuracy of the optical fractionator results (West and Gundersen, 1990; Gundersen et al., 1999). The CEs for microglia and astrocyte cell counts are provided in Supplemental Table 1. The estimated total numbers of glial cells were used for statistical comparisons between age groups within each DA subregion, and the cell density (estimated number/mm^3) was used for comparisons between DA subregions within each age group. Use of cell density was necessary for comparisons between anatomical subregions due to the size differences between the vtSN, dtSN, and VTA. On average, tissue sections were 18.07 μm

(SEM ±1.02), 19.40 μm (SEM ±0.31), and 19.28 μm (SEM ±1.06) thick for young, middle-age, and old-age animals.

2.5. Morphology rating

Microglia and astrocytes exhibit morphological characteristics that correlated with functional states that ranged from "resting" to "activated" (Dalmau et al., 1998; Streit et al., 1999; Pekny and Nilsson, 2005). Using HLA-DR and GFAP IHC, microglial and astrocyte morphologies were determined independently in each midbrain DA neuron subregion, and a qualitative rating for each stain in each subregion was given by a blinded rater.

A rating scale for microglia was developed using similar criteria as those previously published (Streit and Sparks, 1997; Hurley et al., 2003). Resting microglia are ramified with little to no cytoplasmic staining and numerous fine lightly stained fibers. A (—) rating indicates the majority of microglia are resting (Figure 1A). An intermediate stage of activation is known as "hyper-ramified" microglia, which have a ramified morphology similar to resting microglia, but with increased immunoreactivity for HLA-DR in the cell body and fibers (Figure 1B). A (+) rating indicates the presence of numerous hyper-ramified and none or few microglia exhibit signs of advanced activation. In advanced stages of activation, microglia take on a macrophage-like morphology with larger cell bodies that are intensely immunoreactive with few short, thick, and strongly labeled processes (Figure 1C). Advanced stages of activation also are associated with the presence of multicellular clusters (Figure 1D). A (++) rating indicates the presence of numerous hyper-ramified microglia in addition to the emergence of numerous fully activated microglia morphologies (Figure 1B-D). Lastly, a (+++) rating indicates the majority of microglia exhibit morphological characteristics of advanced activation (Figure 1C and D).

Resting astrocytes have little cytoplasmic staining and fine lightly stained fibers. A rating of (—) indicates the majority of astrocytes were in a resting state (Figure 2A). Reactive astrocytes become hypertrophic exhibiting increased cytoplasmic GFAP staining and thicker more intensely stained processes. A rating of (+) indicates the presence of numerous astrocytes exhibiting an intermediate level of hypertrophy (Figure 2B). A (++) rating indicates the majority of astrocytes are fully reactive, which is characterized by further enlargement of the cell body containing strong cytoplasmic staining with thick and shorter processes strongly labeled with GFAP (Figure 2C).

2.6. Semi-quantitative Immunofluorescence

To determine the relative fluorescence intensity of HLA-DR and GFAP, a 1-in-24 series of tissue was stained using triple-label immunofluorescence for HLA-DR, GFAP, and TH. Tissue sections were rinsed, incubated in blocking serum for 1 hour, and then incubated in the primary antibody solution for 72 hrs at 4° C. The primary antibody solution consisted of mouse anti-HLA-DR (1:100; IgG_{2b}; same as above), rabbit anti-GFAP (1:2,000; same as above), and mouse anti-TH (1:1,400; IgG_1; same as above) diluted in 2% GS/TBS. The tissue was then rinsed, incubated in a secondary antibody solution for 1 hour, rinsed, mounted on a microscope slide and allowed to air-dry. The secondary antibody solution consisted of goat anti-mouse IgG_{2b} conjugated with Alexa Fluor® 488 (HLA-DR), goat anti-rabbit IgG conjugated with Alexa Fluor® 555 (GFAP), and goat anti-mouse IgG_1 conjugated with Alexa Fluor® 647 (TH) antibodies diluted 1:400 in 2% GS/TBS. Once the sections were dry, autofluorescence was blocked using autofluorescent eliminator reagent (Chemicon, 2160) following the same protocol as previously published (Kanaan et al., 2007). Sections were coverslipped using Gel/Mount (Biomeda, M01, lot 21433). Penetration of immunofluorescence staining for HLA-DR and GFAP throughout the entire z-axis of the tissue sections was confirmed prior to analysis.

Relative fluorescence intensity of HLA-DR and GFAP staining was performed using a three-laser scanning Olympus confocal microscope equipped with Fluoview version 4.3 software (Olympus America) and argon and helium/neon ion lasers. HLA-DR immunofluorescence was detected using excitation of 488nm and emission filter of 505-525nm. GFAP immunofluorescence was detected using excitation of 543nm and emission filter of 560-600. TH immunofluorescence was detected using excitation of 633nm and emission filter of 660-infared. It should be noted that autofluorescence did not contribute to the fluorescence as it was effectively blocked (as described above), which was confirmed in control sections.

Images for measuring the intensity of individual HLA-DR+ microglia were taken at 20x magnification, an image resolution of 1,024 × 768, and saved in the multi-tiff format in Fluoview. Care was taken to accurately outline the cell body and processes of individual microglia and the average pixel intensity was measured. In addition, 20X magnification was necessary to visualize resting microglia. Images for measuring regional GFAP fluorescence intensity were taken at 10x magnification. Regional fluorescence intensity was measured for astrocytes since they had many long processes spanning numerous levels of the z-axis, and astrocyte fibers were distributed in a relatively even and extensive manner in the neuropil (see Figure 7). For GFAP intensity, average pixel intensity was measured over the entire field of view in each image. Regional analysis of microglia was not feasible since microglia were not evenly distributed within midbrain subregions (see Figure 4). Images for microglia and astrocyte analysis were taken throughout the entire region (vtSN, dtSN, and VTA) within each section through the rostral-caudal extent of the nigra and used for analysis. All confocal settings (e.g. PMT, gain, offset, laser intensity, confocal aperture, and scan speed) were maintained between each animal and the sequential scan mode was used to ensure cross-over between fluorophores did not occur. ImageJ version 1.36b software (National Institutes of Health, Bethesda, MD) was used to measure pixel intensity. This analysis measures the average pixel intensity ranging from 0 (black) to 4,095 (white). As glial cells are present throughout the brain, background levels of staining were determined in areas of the cerebral peduncle where no staining was present (“blank” areas between glial cell bodies and fibers). Background levels were subtracted from the measurements made in the vtSN, dtSN, and VTA. It should be noted that these methods allow measurements of relative differences in fluorescence intensity, but do not allow direct measurements of absolute antigen levels in the tissue. Unfortunately, the current tissue resource does not lend itself to biochemical analyses (e.g. protein concentration or mRNA levels). Future studies will be necessary to directly measure absolute protein levels.

2.7. Statistics

Nonparametric statistical tests were used to compare groups (Kanaan et al., 2007). The Kruskal-Wallis one-way analysis of variance (ANOVA) on ranks test was used to compare differences between age groups. The Spearman rank correlation was used to evaluate correlations with chronological age. The Friedman repeated measures ANOVA on ranks test was used for comparisons between the three DA subregions within each age group. When appropriate, the Dunn’s method was used for post-hoc comparisons. $P \leq 0.05$ was considered statistically significant. All statistics were done using SigmaStat version 3.0.1 software (SPSS, Chicago, IL).

3. Results

3.1. Microglia in the aging midbrain

3.1.1. Number of microglia does not change during normal aging in the SN and VTA—Stereological cell counting was used to determine whether the number of microglia expressing HLA-DR changes during normal aging in the DA subregions of the midbrain. When differences between age groups were evaluated using ANOVA on ranks tests, no significant

changes in microglia number were found within the vtSN, dtSN, or VTA ($p > 0.05$). Similarly, no significant correlations between chronological age and microglia number in any DA neuron subregion were observed ($p > 0.05$), but a trend toward increased numbers of microglia in all three subregions was found (vtSN: $p = 0.15$, dtSN: $p = 0.06$, and VTA: $p = 0.07$; Figure 3A-C). Microglia density was similar between all three subregions in all three age groups ($p > 0.05$; Figure 3D). The photomicrographs in Figure 3 (E-G) illustrate the number of HLA-DR + microglia in the midbrain of young, middle-age, and old-age animals. Obvious changes in level of HLA-DR-ir and morphology occur with advancing age, but the number of microglia does not significantly increase.

3.1.2. Microglial HLA-DR fluorescence intensity in the ventral midbrain increases during normal aging in a region-specific pattern—To determine changes in HLA-DR in microglia, the fluorescence intensity of individual microglia was measured. There was a significant correlation between increased intensity of HLA-DR staining in microglia and increasing age in both nigral regions, the vtSN and dtSN ($p < 0.05$; Figure 4A and B). In contrast, aging was not associated with a significant increase in HLA-DR fluorescence in microglia of the VTA ($p > 0.05$; Figure 4C). In all three age groups, microglia in the vtSN had the highest levels of HLA-DR fluorescence (Figure 4D). In young animals, the vtSN microglia were more intense than those in the dtSN ($p = 0.028$), in middle-aged animals microglia were more intense in the vtSN compared to both the dtSN and VTA ($p = 0.008$), and in old-aged animals HLA-DR fluorescence in microglia of the vtSN was greater compared to those in the VTA ($p = 0.024$). Increased HLA-DR fluorescence intensity in the vtSN with advancing age is depicted in Figure 4 (E – young and F – old-age). In contrast, note the lack of an age-related increase in microglia of the VTA (G – young and H – old-age). These data suggest microglia in both nigral regions undergo changes associated with ongoing activation during normal aging, while those in the VTA do not undergo such changes. Furthermore, the reactivity of microglia in the degeneration vulnerable vtSN, as indicated by HLA-DR fluorescence intensity, is exaggerated compared to the resistant dtSN and VTA.

3.1.3. Microglia undergo morphological changes during normal aging in a region-specific pattern—To evaluate the degree of reactivity in HLA-DR+ microglia, as indicated by morphological changes, morphology was qualitatively rated (Table 1). In general, there appeared to be an age-related change in microglia morphology from a resting state to more activated morphologies in all DA subregions. In young animals, microglia exhibited morphological profiles indicative of a resting state, while some hyper-ramified microglia were seen (Figure 5A-A”). There was not a difference between morphological characteristics of microglia in the vtSN, dtSN, and VTA of young animals (Figure 5A-A”). With advancement into middle-age, there was an increase in microglia exhibiting more activated morphologies (Figure 5B-B”). In the vulnerable vtSN region, the majority of microglia showed morphological characteristics consistent with mild reactivity (hyper-ramified), and one animal contained microglia with characteristics of advanced activation in the vtSN (Figure 5B). In contrast, in the two resistant regions (dtSN and VTA) microglia were similar to those in young animals with both resting and slightly reactive morphologies (Figure 5B” and B”). By old-age, there was a ubiquitous presence of mildly reactive microglia in all three subregions (Figure 5C-C”). Interestingly, in the vtSN of the oldest animal (#6257, 29 yrs), the majority of microglia exhibited morphologies associated with the most advanced states of activation. These data indicate normal aging is associated with morphological shifts in microglia from resting states to activated states, and specifically, the vtSN region contains microglia in advanced stages of activation. Furthermore, morphological changes support the differences in HLA-DR intensity, which suggests there is a state of chronic mild inflammation occurring in the midbrain during normal aging that is exaggerated in the vulnerable vtSN region.

3.2. Astrocytes in the aging midbrain

3.2.1. Astrocyte number does not change during normal aging in the SN and VTA—Unbiased stereological estimates of the number of GFAP+ astrocytes were performed to assess astrocyte proliferation in DA subregions of the midbrain during normal aging. There were no statistical differences in any of the analyses used to compare astrocyte number between age groups ($p > 0.05$), to correlate astrocyte number with chronological age ($p > 0.05$; Figure 6A-C), or to compare astrocyte density between DA neuron subregions ($p > 0.05$; Figure 6D). The stability of astrocyte number as a function of age in midbrain DA subregions is represented in the photomicrographs of the VTA from a young and old-age animal (Figure 6E and F). These data suggest that astrocytes do not proliferate or migrate into the midbrain DA subregions during normal aging.

3.2.2. Regional GFAP fluorescence intensity does not change during normal aging in the SN and VTA—To determine whether the level of GFAP fluorescence changes during normal aging in midbrain DA subregions, regional fluorescence intensity measurements were used. GFAP fluorescence intensity was not different between age groups in any of the subregions ($p > 0.05$). Similarly, GFAP fluorescence was not significantly correlated with chronological age in the vtSN, dtSN, and VTA ($p > 0.05$; Figure 7A-C). In all three age groups, the dtSN had the lowest levels of GFAP fluorescence (Figure 7D). Specifically, in young animals the dtSN had lower levels compared to the VTA ($p = 0.028$), in middle-age animals the dtSN was lower than both the vtSN and VTA ($p = 0.008$), and in old-age animals the dtSN was reduced compared to the vtSN ($p = 0.024$). Figure 7E-G illustrates GFAP fluorescence in midbrain DA subregions of a middle-age animal. Lower GFAP fluorescence in the dtSN is readily appreciable, and is mostly due to the presence of more strongly labeled GFAP+ fibers in the vtSN (E) and VTA (G) compared to the dtSN (E). These data indicate that the level of GFAP is similar across age groups and that the dtSN appears to have the lowest levels of GFAP fluorescence. Thus, changes in GFAP-ir are not consistent with an involvement of reactive astrocytes in regional susceptibility or resistance to degeneration among DA neurons.

3.2.3. Astrocytes undergo morphological changes during normal aging—A qualitative rating scale was used to determine the morphological changes in GFAP+ astrocytes (Table 2). The morphology of astrocytes was consistent across the three subregions in most of the animals. In general, there was not a dramatic change in astrocyte morphology associated with advancing age in any region. Reactive astrocytes were seen only in some of the middle-aged animals. Thus, there may be an inverted U-shaped relationship in morphological changes associated with normal aging in the midbrain (Figure 8A-A”). With progression into middle-age, astrocytes exhibited a shift in morphology to an intermediate degree of reactivity in some animals (Figure 8B-B”). Only in the middle-aged group did an animal have a rating of (++), which indicates the presence of mildly hypertrophic astrocytes (same as in a + rating) as well as fully reactive astrocytes. By old-age, the astrocytes shifted back to a resting morphology similar to astrocytes in young animals (Figure 8C-C”). Thus, aging is associated with hypertrophy of astrocytes in middle-aged animals, but by old-age, the astrocytes return to a resting state similar to astrocytes in young monkeys. These data do not support an involvement of age-related astrocytosis in regional differences to susceptibility among DA subregions.

3.2.4. Effects of aging on GFAP+ astrocytes in other brain regions—To confirm our animals follow the previously reported patterns of age-related changes in astrocytes in other brain regions, we qualitatively analyzed GFAP+ astrocytes in the cortex, putamen, globus pallidus, and hippocampus of young, middle-age, and old-age animals (Supplemental Figure 1). The astrocytes in aged animals appear to be greater in number, larger and more darkly stained, with thicker processes emanating from the cell bodies. Moreover, GFAP+ fiber content

in the neuropil is increased in aged animals. These data confirm previous observations and strengthen the validity of the novel findings in midbrain subregions.

4. Discussion

This is the first report on age-related changes in microglia and astrocytes in specific DA neuron subregions of the naïve rhesus monkey midbrain. Previously, we have shown DA neurons in these subdivisions undergo region-specific changes in intrinsic cellular markers that are associated with their degree of susceptibility to degeneration (Kanaan et al., 2007). Here we expand these results to include factors outside DA neurons, showing changes in the glial environment that may influence vulnerability of vtSN DA neurons to degeneration and resistance of dtSN and VTA DA neurons. The intensity of HLA-DR fluorescence in microglia increased with advancing age in the vtSN and dtSN, but not the VTA. Morphological changes in microglia suggest microglia become reactive with advancing age in all three subregions. Importantly, microglia in the vulnerable vtSN region exhibited morphological characteristics consistent with advanced stages of activation. In contrast, microglia in resting and intermediate stages of activation were found in the resistant dtSN and VTA. Our cell counts, intensity measures of GFAP fluorescence, and morphology data suggest age-related changes in astrocytes do not contribute in any obvious way to regional differences in susceptibility among DA neurons. It must be acknowledged that our findings may be specific for nonhuman primates and are limited by the low number of subjects available for study. In this regard, statistically significant findings likely represent robust changes, but subtle changes may have remained undetected.

The current study shows that normal aging was associated with changes in microglia consistent with chronic inflammation in DA midbrain subregions, with the vtSN being most affected. We did not detect statistically significant increases in the number of microglia in DA subregions. These data are similar to those reported by Oguara and colleagues (1994), who did not find a significant change in numbers of microglia of the SN when comparing young to middle-aged rats (Ogura et al., 1994). Previous work has established an age-related activation of microglia in numerous brain regions (white matter tracts, hippocampus, striatum, and globus pallidus) and multiple species (rodents, monkeys, and humans), and suggests white matter tracts are most severely affected with advancing age (Luber-Narod and Rogers, 1988; Mattiace et al., 1990; Peters et al., 1991; Gordon et al., 1992; Ogura et al., 1994; Sheng et al., 1998; Sheffield and Berman, 1998; Sloane et al., 1999; Morgan et al., 1999). Consistent with activation of microglia during normal aging, we detected a significant increase in level of HLA-DR staining in the vtSN and dtSN, but not the VTA. The use of MHC-II markers for identifying reactive microglia is particularly useful since an upregulation of these glycoproteins is an integral part of immune functions of activated microglia, such as antigen presentation (Aloisi, 2001). HLA-DR levels in vtSN microglia were significantly more intense compared to those in the resistant dtSN and VTA. Consistent with age-related and region-specific patterns of microglial activation, the morphology of microglia was associated with advancing stages of activation with advancing age in all midbrain subregions. Microglia in the vtSN consistently exhibited morphological characteristics of advanced activation stages, while microglia in the resistant dtSN and VTA always exhibited either resting or mildly activated morphologies. The SN normally has one of the highest concentrations of microglia in the brain (Lawson et al., 1990) and it has been postulated that simply having more microglia enhances the vulnerability of surrounding neurons following an inflammation-inducing insult (Kim et al., 2000). While the number of microglia was not different between midbrain subregions in our monkeys, the changes in HLA-DR intensity and morphological characteristics indicate age-related inflammation occurs in the DA subregions of the midbrain, and is exaggerated in the vtSN. This suggests that the increase of activated microglia, as defined via phenotype and

morphology, in the vtSN may contribute to the greater relative vulnerability of these DA neurons to degeneration.

The role of microglial activation as a neuroprotective or neurodestructive process remains complex and is most likely context dependent (e.g. acute vs. chronic inflammation) (van Rossum and Hanisch 2004; Vilhardt 2005). Indeed, microglia have been shown to produce neurotrophic factors (e.g. brain derived neurotrophic factor and glial cell line derived neurotrophic factor), which could enhance neuronal survival and plasticity (Batchelor et al. 1999). On the other hand, many studies have indicated that microglial activation and subsequent production of pro-inflammatory cytokines, free radicals, and phagocytic activity may be harmful to neurons (Kim and Joh 2006). Inflammation and microglial activation are thought to play an important role in PD (Hartmann et al. 2003; Kim and Joh 2006; McGeer et al. 1988). However, a point of continuing contention is whether microglial activation actively participates in DA neuron degeneration or represents a response to damage. Recent work by Saint-Pierre and colleagues, has demonstrated that microglial activation precedes DA neuron loss in an animal model of PD (Saint-Pierre et al. 2006). Moreover, numerous studies have shown treatment with anti-inflammatory agents (e.g. minocycline and dexamethasone) that reduce microglia activation, elicit enhanced neuronal survival following an insult (Barcia et al. 2003; Herrera et al. 2005). Perhaps the presence of activated microglia in the aging vtSN renders this region more sensitive to ongoing pathological changes, neurotoxic insults, and other inflammation-inducing events. Many studies have implicated microglial production of tumor necrosis factor-α, interleukin-1β, interferon-γ, nitric oxide, and reactive oxygen species, among others, in the toxic effects of microglial activation (Kim and Joh 2006; Nagatsu and Sawada 2005). Further exploration of the profile of factors (e.g. cytokines, chemokines, free radicals, neurotrophic factors, and anti-oxidants) produced by activated microglia in specific DA subregions during normal aging is warranted.

We were unable to discern significant changes in astrocytes (number, GFAP fluorescence, and morphology) of the midbrain that would suggest age-related astrocytosis is associated with regional differences in vulnerability of DA neurons. There is conflicting data in the literature as to whether astrocyte number changes with advancing age. For instance, age-related increases in astrocyte number have been documented in the cerebral cortex (Vaughan and Peters, 1974; Peinado et al., 1997; Peinado et al., 1998), the molecular layer of the dentate gyrus (Pilegaard and Ladefoged, 1996), the dorsal lateral geniculate nucleus (Satorre et al., 1985), and the neostriatum (Sturrock, 1980). In contrast, other studies were unable to detect significant changes in astrocyte number in cerebral cortex (Hansen et al., 1987; Peters et al., 1991; Peters et al., 1994) and the hippocampus (Landfield et al., 1977; Geinisman et al., 1978; Landfield et al., 1978). It is likely that changes in astrocyte numbers are specific to the regions being studied, and the method used to identify astrocytes. The majority of studies use GFAP to assess astrocyte reactivity. However, using GFAP to determine astrocyte number may be inaccurate. Gordon and coworkers (1997) demonstrated that the number of GFAP+ striatal astrocytes increases after a 6-OHDA lesion of the medial forebrain bundle, but when glutamine synthetase+ and S100+ (additional astrocyte markers) astrocytes are quantified there is not a change in cell number (Gordon et al., 1997). These data suggest that an increase in GFAP+ astrocyte number may be due to detection of previously non-detectable astrocytes, while the number of resident astrocytes does not change. Other measures of astrocyte reactivity (e.g. increased GFAP protein, increased expression of GRAP mRNA, and morphological changes) more clearly and reliably indicate astrocyte reactivity, since they are based on individual cell characteristics and consistently occur as a function of reactivity. Importantly, the absence of differences in GFAP fluorescence and morphological changes in the current study further support the conclusion that astrocyte activation does not occur readily in midbrain DA subregions during normal aging and does not play a major role in regional differences in susceptibility to degeneration among DA neurons. These data are consistent with previous reports demonstrating an absence of age-

related changes in the level of GFAP protein and astrocyte morphology in select brain regions, such as the forebrain of rodents and cortex of humans (Landfield et al., 1977; David et al., 1994). Thus, it appears that age-related astrocytosis is not a ubiquitous event affecting all regions of the brain equally.

It must be acknowledged that our results conflict with numerous studies clearly showing astrocyte hypertrophy with advancing age in multiple brain regions and multiple species. For instance, increases in GFAP mRNA, GFAP protein, area fraction of GFAP staining, and transition to more activated morphologies have consistently been demonstrated in the cortex, hippocampus, striatum, globus pallidus, and cerebellum, among other regions (Landfield et al., 1977; Geinisman et al., 1978; Lindsey et al., 1979; Bjorklund et al., 1985; Beach et al., 1989; Finch and Morgan, 1990; Goss et al., 1991; O'Callaghan and Miller, 1991; Bronson et al., 1993; Nichols et al., 1993; Goss and Morgan, 1995; Morgan et al., 1999). Importantly, none of these previous studies have analyzed age-related changes in the midbrain of nonhuman primates. Changes in the substantia nigra only were briefly described in two studies. Intense GFAP-ir was noted in the substantia nigra of aged humans (Beach et al., 1989) and low levels of GFAP staining were noted in the midbrain of aged mice (Bronson et al., 1993). Age-related changes in astrocytes are thought to be in response to degenerative events, such as synaptic loss and perhaps low levels of neuronal attrition in select areas (Goss and Morgan, 1995). The underlying reasons for a lack of age-related changes in astrocytes of the midbrain remain to be determined. Perhaps the degree of age-related cellular dysfunction in the midbrain is not sufficient to induce astrocytosis. Indeed, frank neuronal loss in the SN does not occur as a function of normal aging. Recent work from our groups shows that in response to MPTP, compensatory mechanisms, which may be mediated in part by astrocytes, are reduced in the nigrostriatal system of aged nonhuman primates (Collier et al., 2005; Collier et al., 2007). The general increase in the susceptibility of midbrain DA neurons to degeneration in aged animals may possibly be due, in part, to a reduced compensatory neuroprotective response expressed by astrocytes. Alternatively, age-related changes in oligodendrocytes may be important in understanding the differences in DA neuron susceptibility to degeneration. While oligodendrocytes were not evaluated in these studies, numerous lines of evidence suggest changes in oligodendrocytes may play an important role in degenerative changes during aging and in neurodegenerative diseases (for review see Bartzokis G, 2004). Future studies evaluating the age-related changes in oligodendrocyte number and myelination in midbrain subregions are necessary.

Interestingly, we found an age-related trend in astrocyte morphology from resting in young monkeys, to more hypertrophic in middle-age animals, and back to resting in old-age animals. This inverted U-shape relationship in astrocyte reactivity has not been reported previously, however, no detailed analyses of age-related changes in midbrain astrocytes have been performed previously. In contrast to the inverted U-shaped response of astrocytes in the midbrain, we found age-related hypertrophy of astrocytes followed established patterns of progressive increased astrocyte activation in cortical white matter, putamen, globus pallidus, and dentate gyrus of our monkeys. The implications of these unique results in the midbrain remain to be elucidated, but a failure to sustain astrocyte activation in old-age may enhance the susceptibility to degeneration of DA neurons in the aged midbrain.

The data presented here suggest the glial environment undergoes changes during normal aging and that the degree of these changes differ between DA neuron subregions of the midbrain, particularly in the microglia population. We detected no aging-related increase in the number or activation state of astrocytes across all subregions of SN. This is unlike the age-related astrocytosis that characterizes many other brain regions. Morphological changes in astrocytes support the view that astrocytes may be activated in middle-age, but that this response, be it supportive or damaging, disappears in old age. Thus, our evidence does not suggest that age-

related changes in astrocytes play a major role in regional differences in susceptibility to degeneration among midbrain DA neurons. In contrast, an age-related and region-specific increase in microglial activation was detected. During normal aging, increases in HLA-DR-ir and changes in the morphology of microglia support the view that microglia undergo activation with advancing age, and these changes were exaggerated in the vulnerable vtSN region. These data suggest that a chronic inflammatory state in the aged vtSN may contribute to the enhanced susceptibility to degeneration of DA neurons in this region.

Supplementary Material

Refer to Web version on PubMed Central for supplementary material.

Acknowledgments

We would like to thank Brian Daley for his expert technical assistance. Supported by NIH grant AG17092 (TJC) and the Millennium Scholars Fund at the University of Cincinnati (TJC).

References

Aloisi F. Immune function of microglia. Glia 2001;36(2):165–79. [PubMed: 11596125]

Barcia C, Fernandez Barreiro A, Poza M, Herrero MT. Parkinson's disease and inflammatory changes. Neurotox Res 2003;5(6):411–8. [PubMed: 14715444]

Bartzokis G. Age-related myelin breakdown: A development model of cognitive decline and Alzheimer's disease. Neurobio of Aging 2004;25(1):5–18.

Batchelor PE, Liberatore GT, Wong JY, Porritt MJ, Frerichs F, Donnan GA, Howells DW. Activated macrophages and microglia induce dopaminergic sprouting in the injured striatum and express brain-derived neurotrophic factor and glial cell line-derived neurotrophic factor. J Neurosci 1999;19(5): 1708–16. [PubMed: 10024357]

Beach TG, Walker R, McGeer EG. Patterns of gliosis in Alzheimer's disease and aging cerebrum. Glia 1989;2(6):420–36. [PubMed: 2531723]

Bjorklund H, Eriksdotter-Nilsson M, Dahl D, Rose G, Hoffer B, Olson L. Image analysis of GFA-positive astrocytes from adolescence to senescence. Exp Brain Res 1985;58(1):163–70. [PubMed: 3987847]

Bronson RT, Lipman RD, Harrison DE. Age-related gliosis in the white matter of mice. Brain Res 1993;609(1-2):124–8. [PubMed: 8508295]

Chu Y, Kordower JH. Age-associated increases of alpha-synuclein in monkeys and humans are associated with nigrostriatal dopamine depletion: Is this the target for Parkinson's disease? Neurobiol Dis 2007;25 (1):134–49. [PubMed: 17055279]

Collier TJ, Dung LZ, Carvey PM, Fletcher-Turner A, Yurek DM, Sladek JR Jr. Kordower JH. Striatal trophic factor activity in aging monkeys with unilateral MPTP-induced parkinsonism. Exp Neurol 2005;191(Suppl 1):S60–S67. [PubMed: 15629762]

Collier TJ, Lipton J, Daley BF, Palfi S, Chu Y, Sortwell C, Bakay RA, Sladek JR Jr. Kordower JH. Aging-related changes in the nigrostriatal dopamine system and the response to MPTP in nonhuman primates: Diminished compensatory mechanisms as a prelude to parkinsonism. Neurobiol Dis. 2007

Cotrina ML, Nedergaard M. Astrocytes in the aging brain. J Neurosci Res 2002;67(1):1–10. [PubMed: 11754075]

Dalmau I, Finsen B, Zimmer J, González B, Castellano B. Development of microglia in the postnatal rat hippocampus. Hippocampus 1998;8:458–74. [PubMed: 9825958]

Damier P, Hirsch EC, Agid Y, Graybiel AM. The substantia nigra of the human brain. II. Patterns of loss of dopamine-containing neurons in Parkinson's disease. Brain 1999;122(Pt 8):1437–48. [PubMed: 10430830]

David JP, Fallet-Bianco C, Vermersch P, Frigard B, Di MC, Delacourte A. Normal cerebral aging: study of glial reaction. C R Acad Sci III 1994;317(8):749–53. [PubMed: 7882158]

Fearnley JM, Lees AJ. Ageing and Parkinson's disease: substantia nigra regional selectivity. Brain 1991;114(Pt 5):2283–301. [PubMed: 1933245]

Finch CE, Morgan DG. RNA and protein metabolism in the aging brain. Annu Rev Neurosci 1990;13:75–88. [PubMed: 1691607]

Geinisman Y, Bondareff W, Dodge JT. Hypertrophy of astroglial processes in the dentate gyrus of the senescent rat. Am J Anat 1978;153(4):537–43. [PubMed: 727153]

Gibb WR. Melanin, tyrosine hydroxylase, calbindin and substance P in the human midbrain and substantia nigra in relation to nigrostriatal projections and differential neuronal susceptibility in Parkinson's disease. Brain Res 1992;581(2):283–91. [PubMed: 1382801]

Gibb WR, Lees AJ. Anatomy, pigmentation, ventral and dorsal subpopulations of the substantia nigra, and differential cell death in Parkinson's disease. J Neurol Neurosurg Psychiatry 1991;54(5):388–96. [PubMed: 1865199]

Gordon MN, Myers MA, Perlmutter LS, Morgan DG. Microglia of the aged rat brain. Society for Neuroscience Abstract 1992;18(625.9):1488.

Gordon MN, Schreier WA, Ou X, Holcomb LA, Morgan DG. Exaggerated astrocyte reactivity after nigrostriatal deafferentation in the aged rat. J Comp Neurol 1997;388(1):106–19. [PubMed: 9364241]

Goss JR, Finch CE, Morgan DG. Age-related changes in glial fibrillary acidic protein mRNA in the mouse brain. Neurobiol Aging 1991;12(2):165–70. [PubMed: 2052130]

Goss JR, Morgan DG. Enhanced glial fibrillary acidic protein RNA response to fornix transection in aged mice. J Neurochem 1995;64(3):1351–60. [PubMed: 7861168]

Gundersen HJ, Jensen EB, Kieu K, Nielsen J. The efficiency of systematic sampling in stereology--reconsidered. J Microsc 1999;193(Pt 3):199–211. [PubMed: 10348656]

Hansen LA, Armstrong DM, Terry RD. An immunohistochemical quantification of fibrous astrocytes in the aging human cerebral cortex. Neurobiol Aging 1987;8(1):1–6. [PubMed: 3561661]

Hartmann A, Hunot S, Hirsch EC. Inflammation and dopaminergic neuronal loss in Parkinson's disease: a complex matter. Exp Neurol 2003;184(2):561–564. [PubMed: 14769349]

Herrera AJ, Tomas-Camardiel M, Venero JL, Cano J, Machado A. Inflammatory process as a determinant factor for the degeneration of substantia nigra dopaminergic neurons. J Neural Transm 2005;112(1):111–9. [PubMed: 15599609]

Hirsch EC, Breidert T, Rousselet E, Hunot S, Hartmann A, Michel PP. The role of glial reaction and inflammation in Parkinson's disease. Ann N Y Acad Sci 2003;991:214–28. [PubMed: 12846989]

Hunot S, Hirsch EC. Neuroinflammatory processes in Parkinson's disease. Ann Neurol 2003;53(Suppl 3):S49–S58. [PubMed: 12666098]

Hurley SD, O'Banion MK, Song DD, Arana FS, Olschowka JA, Haber SN. Microglial response is poorly correlated with neurodegeneration following chronic, low-dose MPTP administration in monkeys. Exp Neurol 2003;184(2):659–68. [PubMed: 14769357]

Kanaan NM, Collier TJ, Marchionini DM, McGuire SO, Fleming MF, Sortwell CE. Exogenous erythropoietin provides neuroprotection of grafted dopamine neurons in a rodent model of Parkinson's disease. Brain Res 2006;1068(1):221–9. [PubMed: 16368081]

Kanaan NM, Kordower JH, Collier TJ. Age-related accumulation of Marinesco bodies and lipofuscin in rhesus monkey midbrain dopamine neurons: Relevance to selective neuronal vulnerability. J Comp Neurol 2007;502(5):683–700. [PubMed: 17436290]

Kim WG, Mohney RP, Wilson B, Jeohn GH, Liu B, Hong JS. Regional difference in susceptibility to lipopolysaccharide-induced neurotoxicity in the rat brain: role of microglia. J Neurosci 2000;20(16):6309–16. [PubMed: 10934283]

Kim YS, Joh TH. Microglia, major player in the brain inflammation: their roles in the pathogenesis of Parkinson's disease. Exp Mol Med 2006;38(4):333–47. [PubMed: 16953112]

Landfield PW, Rose G, Sandles L, Wohlstadter TC, Lynch G. Patterns of astroglial hypertrophy and neuronal degeneration in the hippocampus of ages, memory-deficient rats. J Gerontol 1977;32(1):3–12. [PubMed: 830730]

Landfield PW, Waymire JC, Lynch G. Hippocampal aging and adrenocorticoids: quantitative correlations. Science 1978;202(4372):1098–102. [PubMed: 715460]

Lawson LJ, Perry VH, Dri P, Gordon S. Heterogeneity in the distribution and morphology of microglia in the normal adult mouse brain. Neuroscience 1990;39(1):151–70. [PubMed: 2089275]

Lindsey JD, Landfield PW, Lynch G. Early onset and topographical distribution of hypertrophied astrocytes in hippocampus of aging rats: a quantitative study. J Gerontol 1979;34(5):661–71. [PubMed: 469184]

Luber-Narod J, Rogers J. Immune system associated antigens expressed by cells of the human central nervous system. Neurosci Lett 1988;94(1-2):17–22. [PubMed: 3266526]

Mattiace LA, Davies P, Dickson DW. Detection of HLA-DR on microglia in the human brain is a function of both clinical and technical factors. Am J Pathol 1990;136(5):1101–14. [PubMed: 1693471]

McGeer PL, Itagaki S, McGeer EG. Expression of the histocompatibility glycoprotein HLA-DR in neurological disease. Acta Neuropathol (Berl) 1988a;76(6):550–7. [PubMed: 2974227]

Morgan TE, Xie Z, Goldsmith S, Yoshida T, Lanzrein AS, Stone D, Rozovsky I, Perry G, Smith MA, Finch CE. The mosaic of brain glial hyperactivity during normal ageing and its attenuation by food restriction. Neuroscience 1999;89(3):687–99. [PubMed: 10199605]

Nagatsu T, Sawada M. Inflammatory process in Parkinson's disease: role for cytokines. Curr Pharm Des 2005;11(8):999–1016. [PubMed: 15777250]

Nichols NR, Day JR, Laping NJ, Johnson SA, Finch CE. GFAP mRNA increases with age in rat and human brain. Neurobiol Aging 1993;14(5):421–9. [PubMed: 8247224]

O'Callaghan JP, Miller DB. The concentration of glial fibrillary acidic protein increases with age in the mouse and rat brain. Neurobiol Aging 1991;12(2):171–4. [PubMed: 1904995]

Ogura K, Ogawa M, Yoshida M. Effects of ageing on microglia in the normal rat brain: immunohistochemical observations. Neuroreport 1994;5(10):1224–6. [PubMed: 7919169]

Peinado MA, Quesada A, Pedrosa JA, Martinez M, Esteban FJ, Del Moral ML, Peinado JM. Light microscopic quantification of morphological changes during aging in neurons and glia of the rat parietal cortex. Anat Rec 1997;247(3):420–5. [PubMed: 9066920]

Peinado MA, Quesada A, Pedrosa JA, Torres MI, Martinez M, Esteban FJ, Del Moral ML, Hernandez R, Rodrigo J, Peinado JM. Quantitative and ultrastructural changes in glia and pericytes in the parietal cortex of the aging rat. Microsc Res Tech 1998;43(1):34–42. [PubMed: 9829457]

Pekny M, Nilsson M. Astrocyte activation and reactive gliosis. Glia 2005;50(4):427–34. [PubMed: 15846805]

Perry VH, Gordon S. Macrophages and the nervous system. Int Rev Cytol 1991;125:203–44. [PubMed: 1851730]

Peters A, Josephson K, Vincent SL. Effects of aging on the neuroglial cells and pericytes within area 17 of the rhesus monkey cerebral cortex. Anat Rec 1991;229(3):384–98. [PubMed: 2024779]

Peters A, Leahu D, Moss MB, McNally KJ. The effects of aging on area 46 of the frontal cortex of the rhesus monkey. Cereb Cortex 1994;4(6):621–35. [PubMed: 7703688]

Pilegaard K, Ladefoged O. Total number of astrocytes in the molecular layer of the dentate gyrus of rats at different ages. Anal Quant Cytol Histol 1996;18(4):279–85. [PubMed: 8862669]

Saint-Pierre M, Tremblay ME, Sik A, Gross RE, Cicchetti F. Temporal effects of paraquat/maneb on microglial activation and dopamine neuronal loss in older rats. J Neurochem 2006;98(3):760–772. [PubMed: 16893418]

Satorre J, Cano J, Reinoso-Suarez F. Stability of the neuronal population of the dorsal lateral geniculate nucleus (LGNd) of aged rats. Brain Res 1985;339(2):375–7. [PubMed: 4027632]

Sheffield LG, Berman NE. Microglial expression of MHC class II increases in normal aging of nonhuman primates. Neurobiol Aging 1998;19(1):47–55. [PubMed: 9562503]

Sheng JG, Mrak RE, Griffin WS. Enlarged and phagocytic, but not primed, interleukin-1 alpha-immunoreactive microglia increase with age in normal human brain. Acta Neuropathol (Berl) 1998;95(3):229–34. [PubMed: 9542587]

Sloane JA, Hollander W, Moss MB, Rosene DL, Abraham CR. Increased microglial activation and protein nitration in white matter of the aging monkey. Neurobiol Aging 1999;20(4):395–405. [PubMed: 10604432]

Streit WJ, Sparks DL. Activation of microglia in the brains of humans with heart disease and hypercholesterolemic rabbits. J Mol Med 1997;75(2):130–8. [PubMed: 9083930]

Streit WJ, Walter SA, Pennell NA. Reactive microgliosis. Prog Neurobiol 1999;57(6):563–81. [PubMed: 10221782]

Sturrock RR. A comparative quantitative and morphological study of ageing in the mouse neostriatum, indusium griseum and anterior commissure. Neuropathol Appl Neurobiol 1980;6(1):51–68. [PubMed: 7374912]

Teismann P, Schulz JB. Cellular pathology of Parkinson's disease: astrocytes, microglia and inflammation. Cell Tissue Res 2004;318(1):149–61. [PubMed: 15338271]

van Rossum D, Hanisch UK. Microglia. Metab Brain Dis 2004;19(3-4):393–411. [PubMed: 15554430]

Vaughan DW, Peters A. Neuroglial cells in the cerebral cortex of rats from young adulthood to old age: an electron microscope study. J Neurocytol 1974;3(4):405–29. [PubMed: 4373545]

Vila M, Jackson-Lewis V, Guegan C, Wu DC, Teismann P, Choi DK, Tieu K, Przedborski S. The role of glial cells in Parkinson's disease. Curr Opin Neurol 2001;14(4):483–9. [PubMed: 11470965]

Vilhardt F. Microglia: phagocyte and glia cell. IntJBiochemCell Biol 2005;37(1):17–21.

West MJ, Gundersen HJ. Unbiased stereological estimation of the number of neurons in the human hippocampus. J Comp Neurol 1990;296(1):1–22. [PubMed: 2358525]

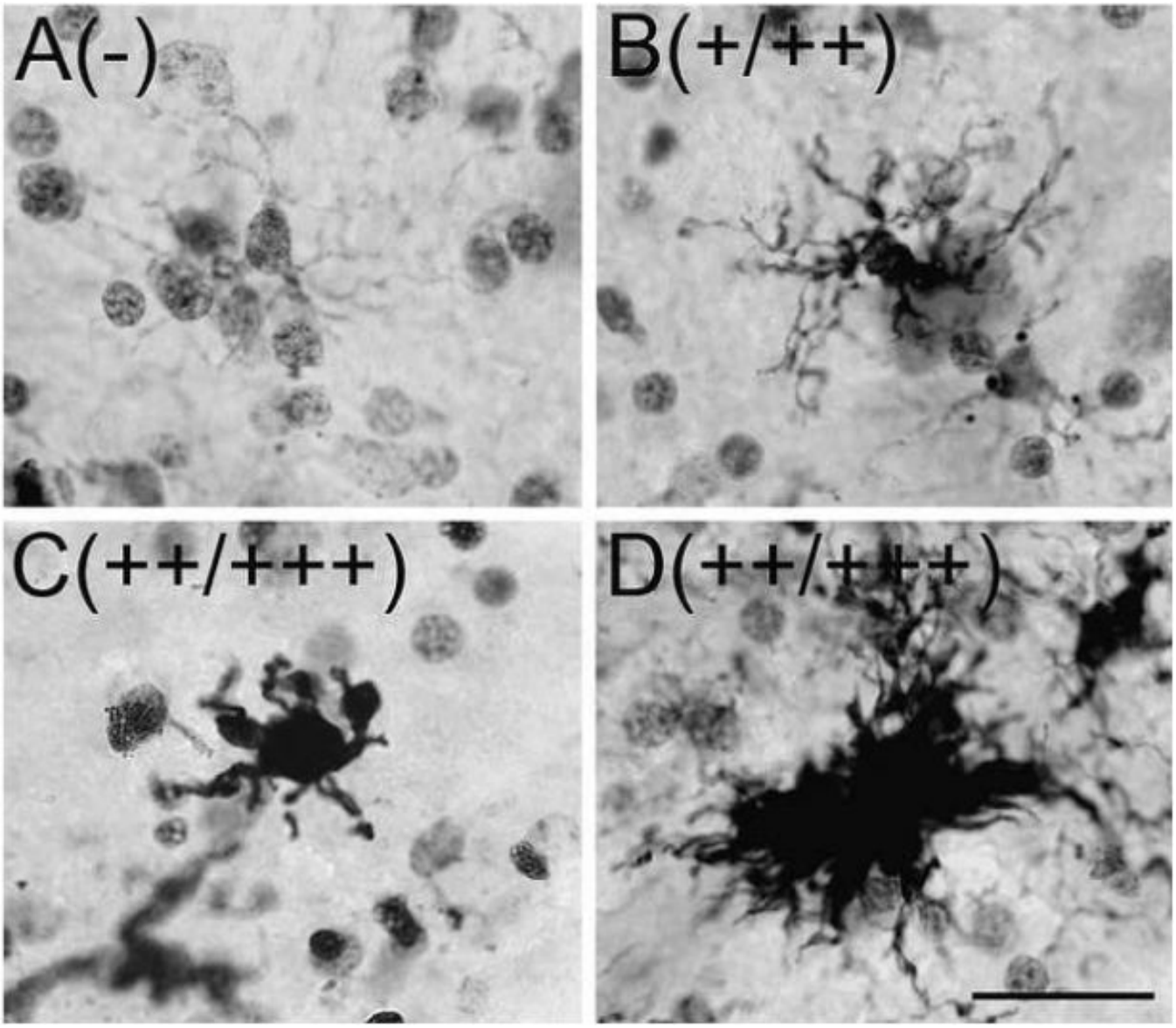

Fig. 1.

HLA-DR+ microglia morphologies in the midbrain. During normal aging, four distinct microglia morphology ratings were observed in the vtSN, dtSN, and VTA using HLA-DR IHC. (A) Resting ramified microglia were characterized by little cytoplasmic staining with fine lightly immunoreactive fibers. A (-) rating indicates the majority of microglia are in a resting state. (B) Hyper-ramified microglia are characterized by an increase in the amount of cytoplasmic staining and more intensely labeled highly branched fibers. A (+) rating indicates the majority of microglia are in the hyper-ramified state, without the presence of many fully activated microglia. (C-D) Advanced stages of activation were characterized by two morphologies. (C) First, macrophage-like microglia are characterized by intense cytoplasmic staining of enlarged cell bodies and short, thick, strongly immunoreactive fibers. (D) Secondly, multicellular clusters are composed of numerous activated microglia. A (++) rating indicates the presence of numerous hyper-ramified and many fully activated microglia. A (+++) rating indicates the vast majority of microglia are in advanced stages of activation. The rating

associated with each photomicrograph is indicated in the parentheses. Scale bar: (A-D) 25 μm.

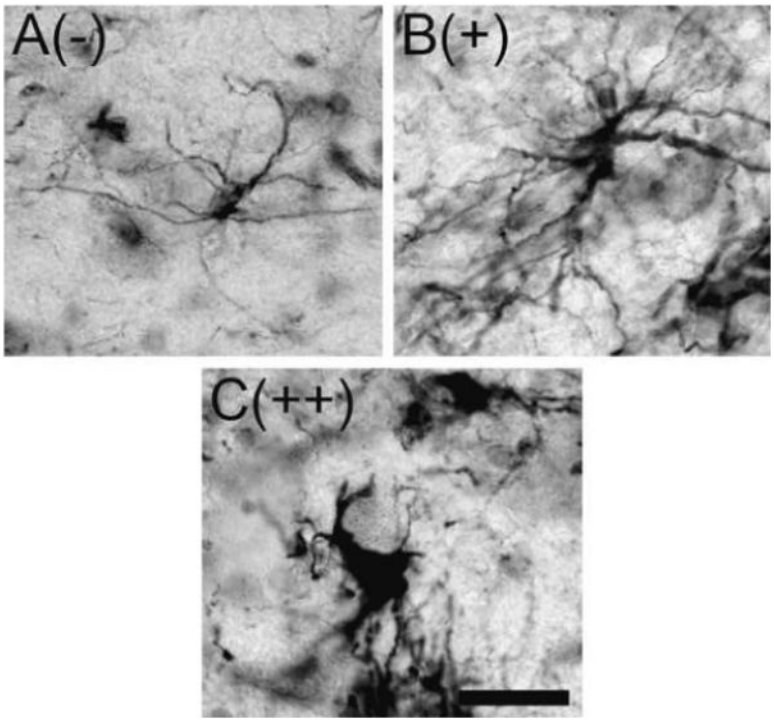

Fig. 2.

GFAP+ astrocyte morphology in the midbrain. During normal aging three distinct astrocyte morphologies were seen using GFAP immunohistochemistry. (A) Resting astrocytes were characterized by fine long fibers emanating from a cell body and low levels of GFAP immunoreactivity in the cytoplasm. (B and C) Reactive astrocytes took on two morphologies. First, astrocytes exhibited an intermediate degree of hypertrophy characterized by increased amounts of cytoplasmic immunoreactivity with thicker more intensely stained fibers (B). Secondly, fully activated astrocytes exhibited enlarged cell bodies with intense cytoplasmic staining and shortened processes with strong labeling for GFAP (C). The rating associated with each photomicrograph is indicated in parentheses. Scale bar: (A-C) 25 μm.

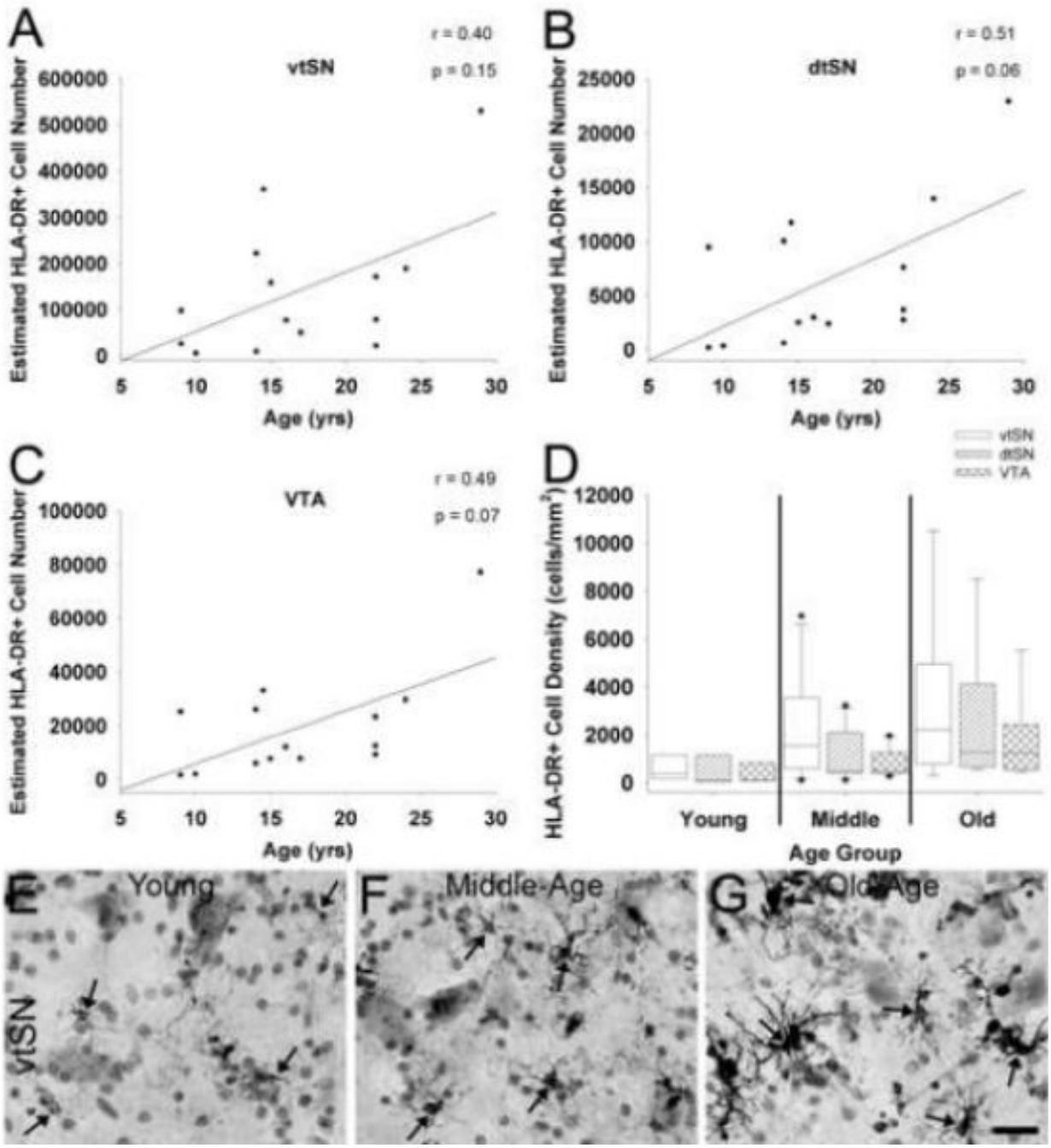

Fig. 3.

Aging is not associated with a significant increase in the number of HLA-DR+ microglia in the midbrain. (A-C) Advancing chronological age was not significantly correlated with numbers of HLA-DR+ microglia, but a trend towards increased numbers of microglia occurred in the vtSN (A), dtSN (B), and VTA (C). (D) When microglia cell density was compared between each subregion, there were not significant differences in any age group. (E-G) The photomicrographs depict the trend towards increased number of microglia in the vtSN with advancing age (E – young, F – middle-age, and G – old-age). Arrows indicate HLA-DR+ microglia. Scale bar: (E-G) 25 μm.

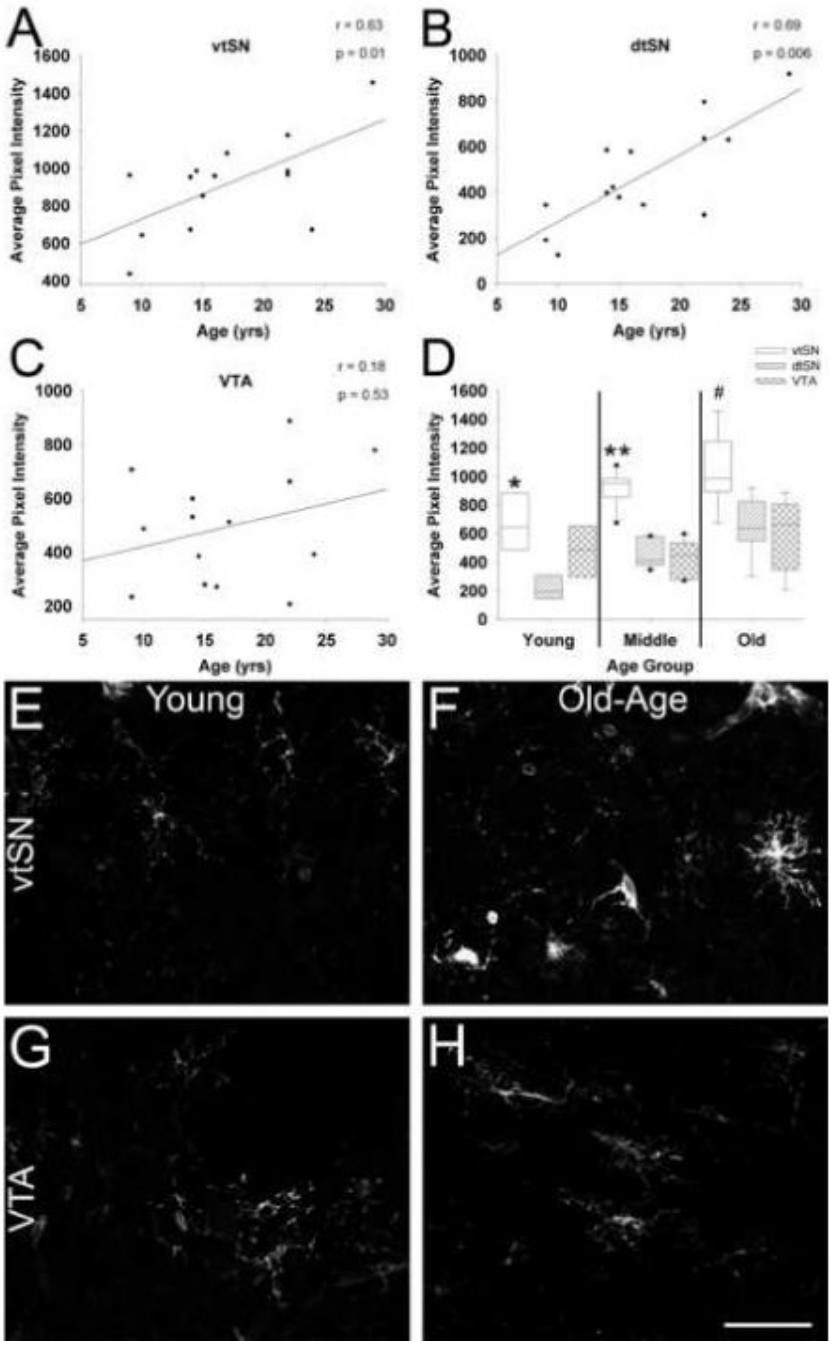

Fig. 4.

The intensity of HLA-DR fluorescence in microglia increases with advancing age in the SN, and is greatest in the vtSN. (A and B) Advancing chronological age is associated with significantly increased HLA-DR fluorescence in microglia of both nigral regions, the vtSN (A) and dtSN (B). (C) No correlation was found between age and microglia intensity in the VTA. (D) Microglia in the vtSN have greater levels of HLA-DR-ir compared to those in the dtSN in young animals (* $p < 0.05$), both the dtSN and VTA in middle-age animals (** $p < 0.05$), and the VTA in old-age animals (# $p < 0.05$). (E-H) The laser confocal microscopic images depict the age-related increase in HLA-DR-ir intensity in the vtSN (E – young and F – old-age). Aging

was not associated with a significant increase in HLA-DR-ir intensity in the VTA (G – young and H – old-age). Scale bar: (E-H) 50 μm.

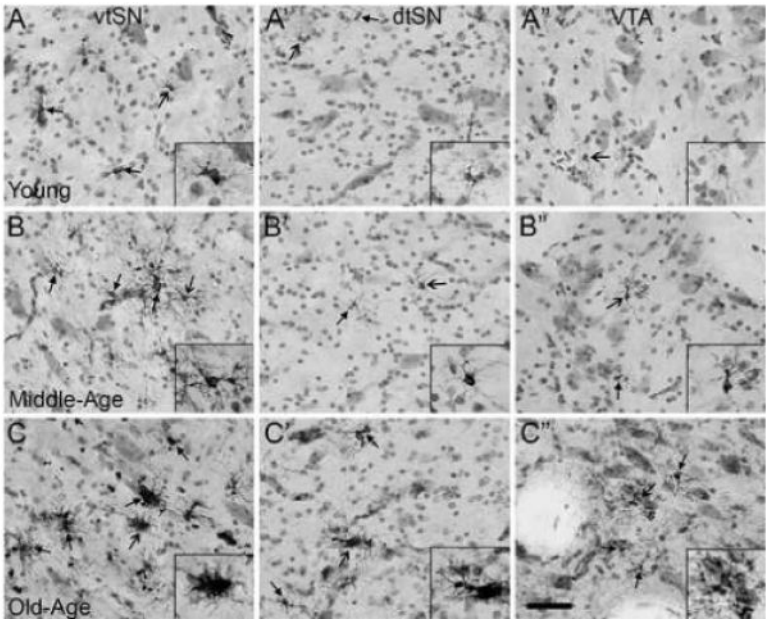

Fig. 5.

Normal aging is associated with a chronic state of moderate inflammation in the midbrain, and the vtSN is most severely affected. (A-A") In young animals, the vtSN (A), dtSN (A'), and VTA (A") have microglia exhibiting resting morphologies (images taken from an animal with − / − / − rating). (B-B") In middle-age animals, the vtSN contains microglia undergoing early stages of activation as evidenced by increased HLA-DR staining and hyper-ramified morphologies (B), while microglia in the dtSN (B') and VTA (B") continue to exhibit resting morphologies (images taken from an animal with + / − / − rating). (C-C") In the midbrain of aged animals, there is a ubiquitous presence of hyper-ramified microglia in the vtSN (C), dtSN (C'), and VTA (C"; images taken from an animal with ++ / + / + rating). (C) Only within the vtSN of an old-age animal (and one middle-age animal – not shown) were the majority of microglia found to exhibit morphological characteristics consistent with advanced stages of activation. Close arrows indicate HLA-DR+ microglia and open arrows indicate cells in insets. Scale bar: (A-C") 50 μm.

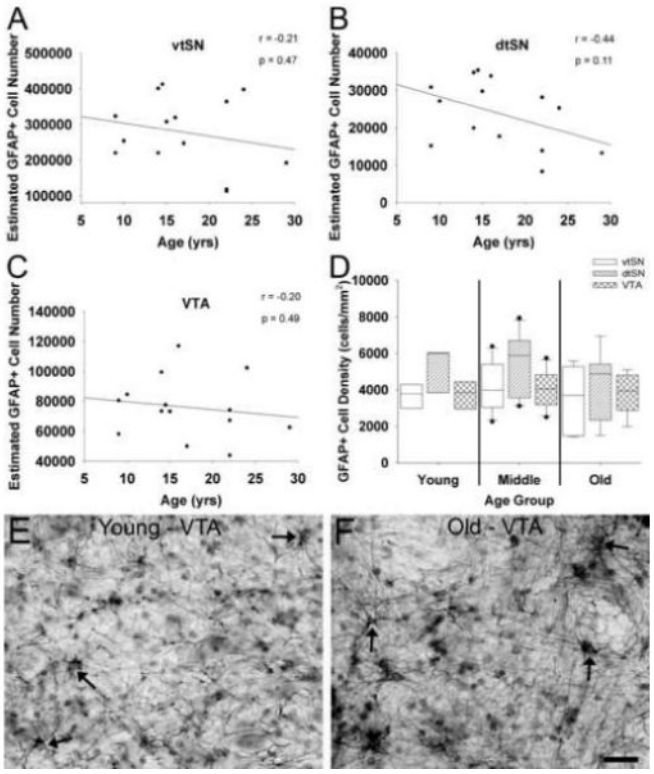

Fig. 6.

Aging is not associated with increased numbers of GFAP+ astrocyte in DA midbrain subregions. (A-C) Increasing chronological age was not significantly correlated with the number of GFAP+ astrocytes in the vtSN (A), dtSN (B), or VTA (C). (D) Astrocyte density was similar in the vtSN, dtSN, and VTA of all age groups. (E and F) The photomicrographs depict no change in astrocyte density in the VTA of a young (E) and old-age (F) animal. Arrows indicate GFAP+ astrocytes. Scale bar: (E and F) 25 μm.

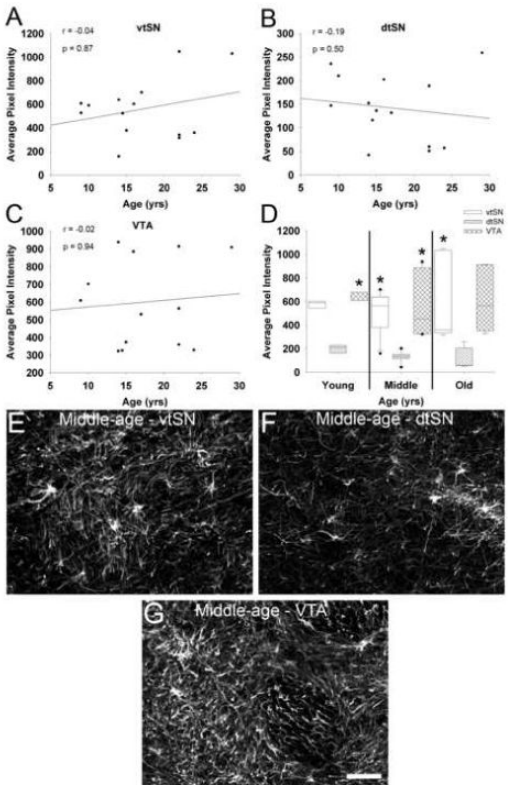

Fig. 7.

GFAP fluorescence did not change during normal aging. (A-C) GFAP fluorescence was not correlated with advancing chronological age in the vtSN (A), dtSN (B), or VTA (C). (D) When DA subregions were compared, the dtSN consistently had the lowest GFAP fluorescence. In young animals, the dtSN was significantly lower than the VTA. In middle-age animals, the GFAP level in the dtSN was significantly lower than both the vtSN and VTA. In old-age animals, GFAP fluorescence was significantly lower in the dtSN compared to the vtSN (* $p < 0.05$ compared to dtSN). (E-G) The laser confocal microscopic images depict higher levels of GFAP fluorescence in the vtSN (E) and VTA (G) compared to the dtSN (F) of a middle-age animal. Scale bar: (E-G) 50 μm.

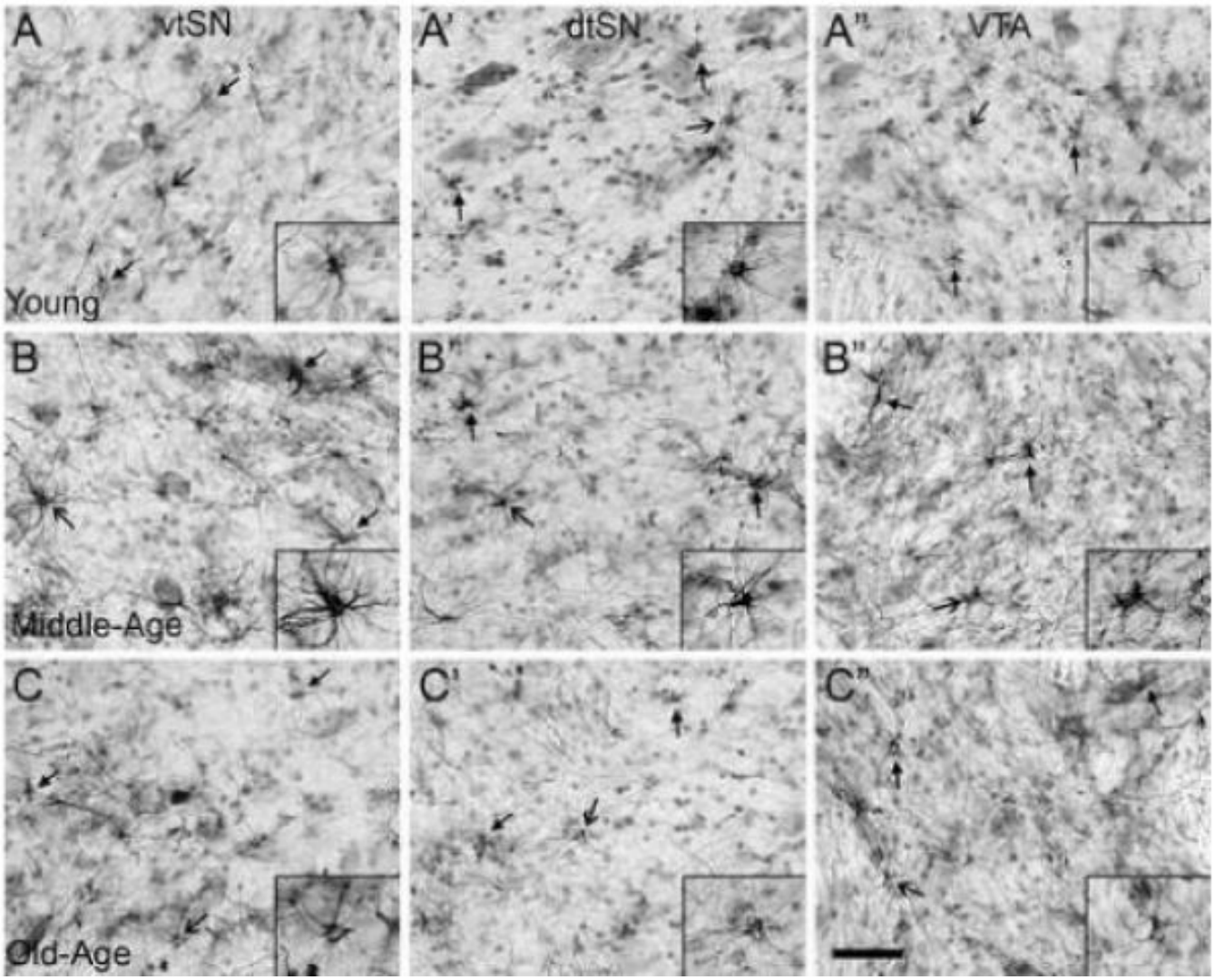

Fig. 8.

In the midbrain, astrocyte activation does not occur in a pattern consistent with an involvement in selective vulnerability of DA neurons to degeneration. (A-C") Generally, the morphology of astrocytes was similar across DA subregions within each age group (young A-A"; middle-age B-B"; and old-age C-C"). However, there was an age-related effect on astrocyte hypertrophy. (A-A") Astrocytes in young animals exhibited morphological characteristics consistent with a resting state (images from an animal with − / − / − rating). (B-B") Advancement into middle-age was associated with a change in astrocyte morphology consistent with moderate levels of reactivity (images from an animal with + / + / + rating). (C-C") By old-age, astrocytes exhibited a shift back to resting states, similar to those in young animals (images from an animal with − / − / − rating). Closed arrows indicate GFAP+ astrocytes and opened arrows indicate the cells in insets. Scale bar: (A-C") 50 μm.

Table 1

Morphological rating of HLA-DR+ microglia in the midbrain during normal aging

			Region		
Age Group	**Animal #**	**Age (yrs)**	**vtSN**	**dtSN**	**VTA**
Young	7043	9	−	−	−
	7044	9	+	+	+
	6480	10	−	−	−
Middle	7048	14	−	−	−
	7080	14	+	−	−
	7050	15	++	+	+
	7049	15	+	−	−
	7108	16	+	+	−
	7109	17	−	−	−
Old	7007	22	+	−	−
	7088	22	+	−	−
	7089	22	++	+	+
	7092	24	++	+	+
	6257	29	+++	++	+

(−) indicates the presence of resting microglia with little to no cytoplasmic immunoreactivity and lightly immunoreactive fine fibers emanating from the cell body (+) indicates numerous hyper-ramified microglia characterized by increased cytoplasmic immunoreactivity and numerous highly branched fibers with moderate to high levels of immunoreactivity, but no or few microglia with morphologies associated with advanced activation

(++) indicates the presence of many hyper-ramified microglia and fully activated microglia characterized by shortened thicker processes, increased cell body size, and strong immunoreactivity, in addition to the emergence of numerous multicellular clusters

(+++) indicates the majority of microglia exhibit morphologies associated with advanced stages of activation, which are macrophage-like and multi-cellular cluster morphologies.

Table 2

Morphological rating of GFAP+ astrocytes in the midbrain during normal aging.

			Region		
Age Group	**Animal #**	**Age (yrs)**	**vtSN**	**dtSN**	**VTA**
Young	7043	9	−	−	−
	7044	9	−	−	−
	6480	10	−	−	−
Middle	7048	14	−	−	−
	7080	14	+	+	+
	7050	15	++	+	+
	7049	15	+	+	−
	7108	16	−	−	−
	7109	17	−	−	−
Old	7007	22	−	−	−
	7088	22	−	−	−
	7089	22	−	−	−
	7092	24	−	−	−
	6257	29	−	−	−

(−) indicates resting astrocytes characterized by little cytoplasmic staining and long thin light-moderately stained processes emanating from the cell body

(+) indicates numerous astrocytes in an intermediate hypertrophic state characterized by increased cytoplasmic staining and thicker darker processes emanating from the cell body

(++) indicates numerous fully hypertrophic astrocytes characterized by increased cell body size with intense staining and shorter thick intensely stained processes emanating from the cell body